
# Adaptive Biocomposite 3D printing Based on Industrial Robotics

Ass. Prof. Federico Rossi
London South Bank University
School of BEA

EPSRC
Engineering and Physical Sciences Research Council

# Executive Summary

The project aim is to prototype a large-scale building component with Additive Manufacturing (AM) robotic process using biopolymers. The pivot point of the research is to establish a Machine Learning (ML) algorithm and workflow to predict/optimize/speed up the printing process using a dataset of information (fiber direction, material defects, temperature, extrusion speed, path planning) and output autonomously optimized solutions for the AM process. With the support of industry partners, we will integrate a fully hybrid manufacturing process depositing the material where needed and machining it to achieve industry tolerance standards. The current project builds upon the experience gained on SCRAM, exploring biopolymers, which can lead to even greater material carbon reductions, and machine learning, which greatly enhance the predictive power of the methodologies employed. The project is spanning across several thematic areas with the aim to increase the possibility to connect design, data, simulation, process prediction and manufacturing for future UK supply chain challenges and to use of Machine Learning (ML) to predict material characterization and 3D printing setting and achieve good structural stability on printed parts.

# Contents

# 1 Management, Procurement

## Management

The project run across (9 Months) comprising several interdependent activities. After procurement (Task 1) across (Month 1), (material characterization, and machine learning algorithm) are heavily interdependent and involve cyclical activities across (Month 2–5) in order to define optimum parameters for the digital manufacturing and design process. This then led into the final activities to produce structural prototypes and finalise report writing across (Month 6–9).

## Procurement

With the support of industry partner, we purchased a batch compound of wood-based biopolymer material, ***DuraSense*** from ***Stora Enso Biocomposites***.

*DuraSense, Stora Enso.*

DuraSense contains a high amount of renewable fibrous material giving diverse advantages:

- Flexibility and excellent tensile properties
- Natural appearance and tactile feeling
- Reduced carbon emissions

Due to the nature of the material with low viscosity, large diameter nozzles are required to be manufactured using tool steel to avoid abrasion during the extrusion process.

The following table illustrates the properties of DuraSense material.

| | Standard | 3D Plus 50 | Unit |
|---|---|---|---|
| Wood content (weight) | - | 50 | % |
| Density | ISO 1183 | 1,10 | g/mm³ |
| Tensile strength | ISO 527-2/50 | 30 | MPa |
| Tensile modulus | ISO 527-2/2 | 2700 | MPa |
| Flexural modulus | ISO 178 | 2800 | MPa |
| Strain at break | ISO 527-2/50 | 7,0 | % |
| Charpy impact strength, 23°C | ISO 179/1eU | 26 | kJ/m2 |

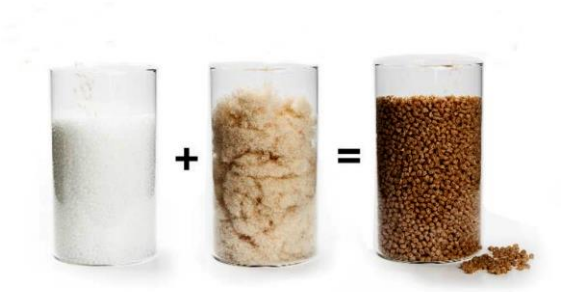

*Stora Enso material, biopolymer with wood fibres.*

**Why biopolymers?**

- Less plastic with post-industrial recycled polymers.
- Reduction of 40% CO2 savings compared to oil-based polymers.
- A true alternative to industrial plastics fossil fuel based.
- Biocomposites as an alternative to traditional material concrete, steel, polymers.
- 51% wood fibers.

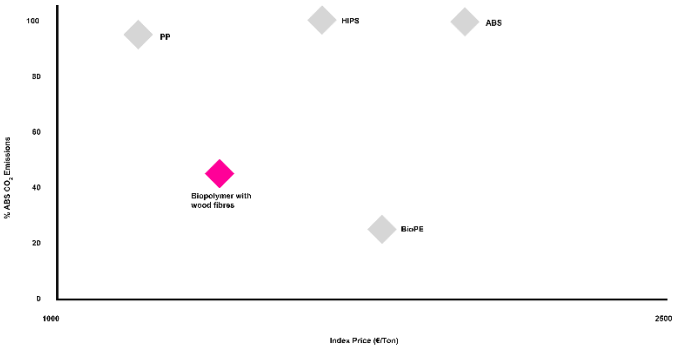


*Stora Enso material comparison, chart.*

# 2 Material Characterization

## Material Test

Tensile coupon specimens conforming to ISO polymer testing standards are printed in various layering orientations (transverse, oblique, longitudinal, and a combination of the three) in order to determine anisotropic material properties. The specimens are defined by seven different patterns: the first set of patterns (A,B,C,D,E) is formed by three layering intensity (4, 6, 12) along the z-axis. Pattern F has 4,8, 12 and pattern CS is printed vertically (through cross-sections) formed by 21 layers on z-axis.

**Original size specimen:** 170 mm *length.* 10mm *(at narrow section)*

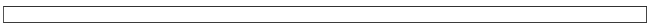

**Original size specimen**: Pattern CS (Cross-section). 170 mm length. 4 mm height.

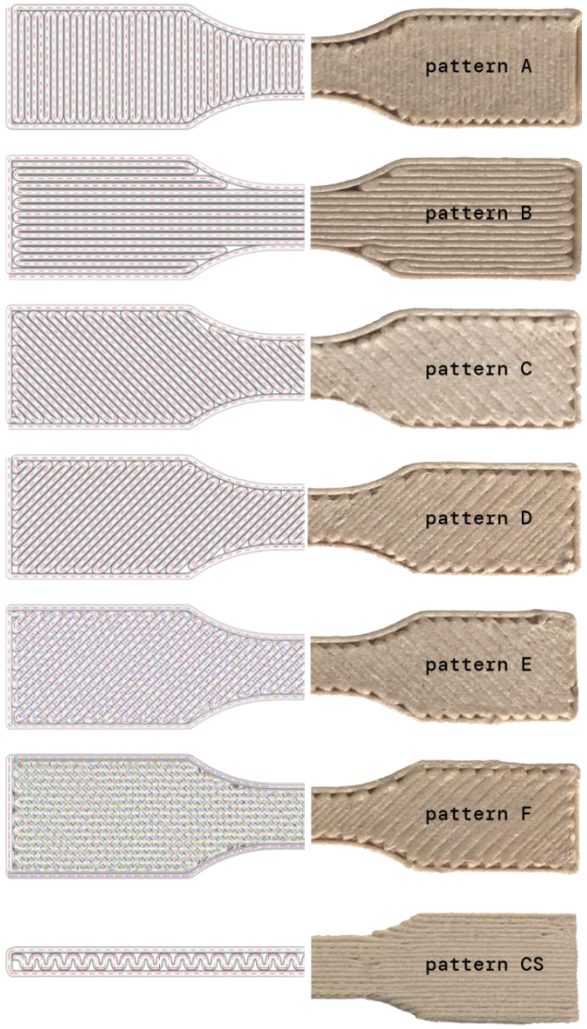


***Fig.1.*** *Digital representation (on the left) and photographs (on the right) of the specimens' layering orientation, top view.*

The printing pathing trajectory is defined by a custom-built G-code in Grasshopper 3D. Testing are conducted at the structure's laboratory at London South Bank University.

```
...
G1 E-0.4 F1800
G1 F900 X214.0 Y124.56 Z2.596 E19.922621
...
```

## Digital Microscope

Advanced digital microscopy equipment available at LSBU is applied to assess the microstructure and micromechanical behaviour of all printed samples. Of particular interest are interlaminar discontinuities and imperfections that occurred during printing, which can considerably affect macroscale mechanical performance.

The specimens are analysed with the aid of a 3D customed printed protractor to control the position of the images.

The aim of the task is to record as much information we can – images – to create a database where ML algorithm can create outputs to influences the operational parameters such as applicator nozzle diameter, melting temperature and deposition rate on the microstructural integrity of the 3D-printed specimens are investigated in detail, which aided the specification of optimum printer operational parameters.

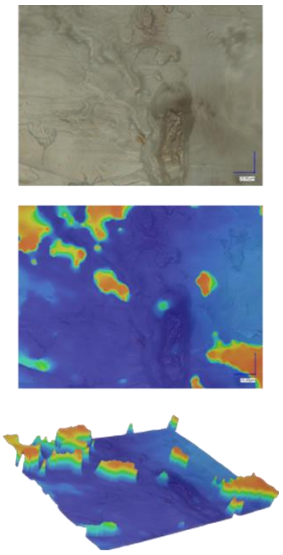

**Fig. 2.** *From top to bottom: Normal Microscope Image, Surface Height Field Image, 3D Iso Surface Height Field Image*

.

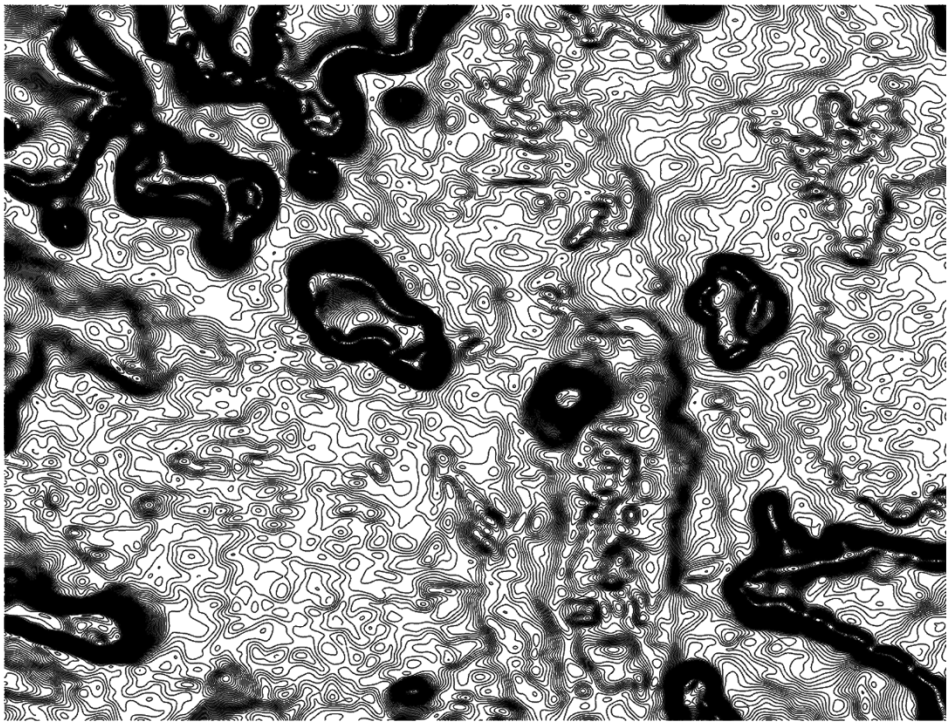

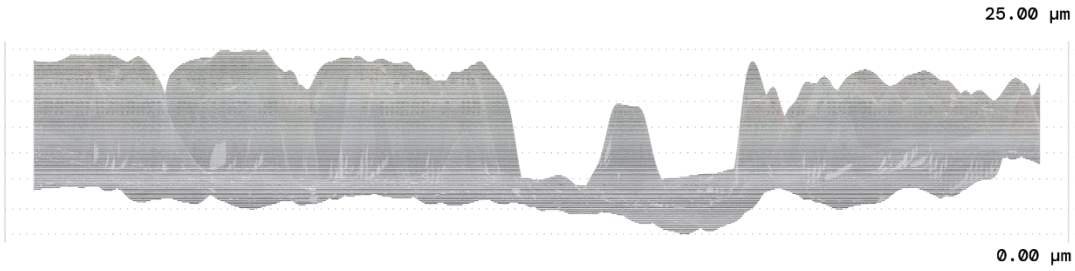


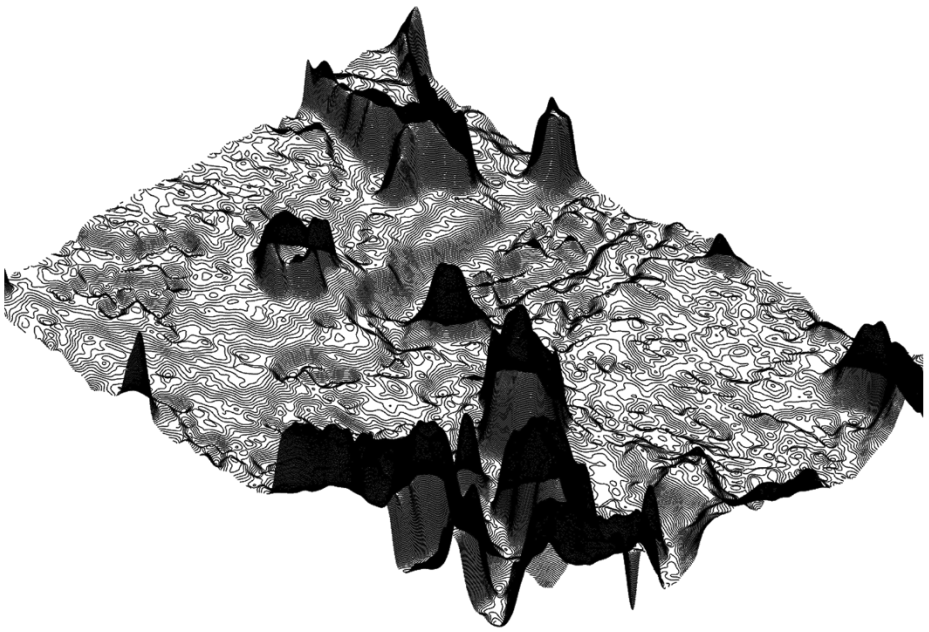

**From top to bottom:**

- Top view of Pattern A (longitudinal), position 1, Section
- Elevation, Sections
- ISO view, Sections

# 3 Machine Learning Algorithm, Digital Manufacturing Process

## Machine Learning Algorithm

Topological optimization supported by finite element analysis in Abaqus analysis software is utilized to define the geometry of specimens – this process is fundamentally dependent on accurate material data available from material test.

Firstly, generic test are applied to a cylindrical geometry in order to prove the feasibility of the interoperability *Grasshopper-Abaqus*.

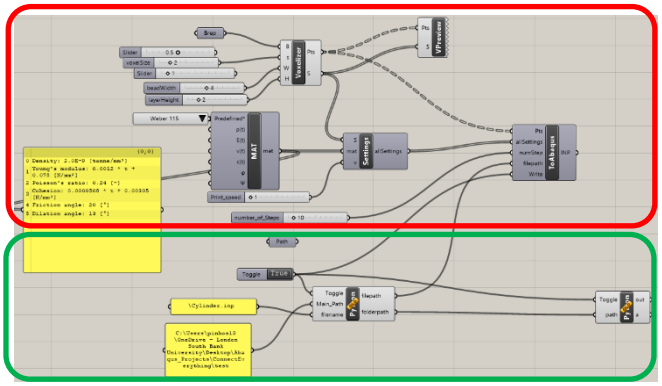

**Fig.3.** *GH script: INP file generator (in red). Run Abaqus and post-process (in green).*

As a result, voxels can be previewed from the GH script:

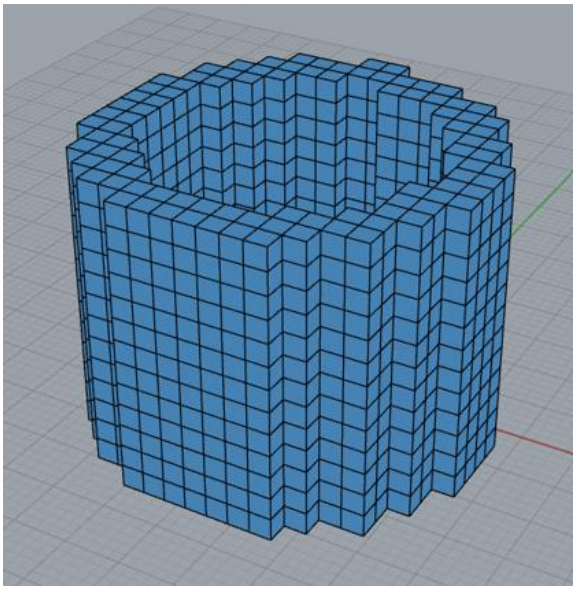

**Fig.4.** *Rhinoceros viewport. Preview of voxels obtained from the GH INP file generator script.*

The following four images show *Von Misses Stress* simulation in *Abaqus* of the holed cylinder modelled in *Rhinoceros*.

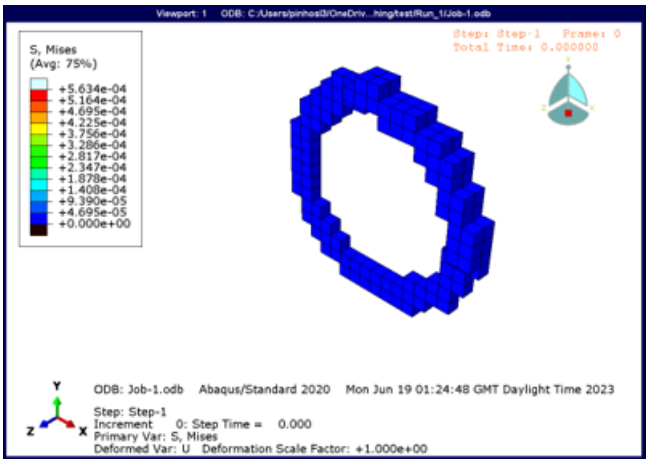


***Frame 1***

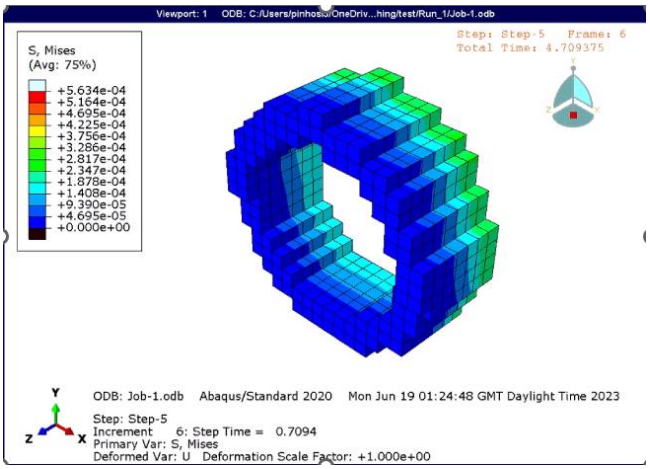


***Frame 2***

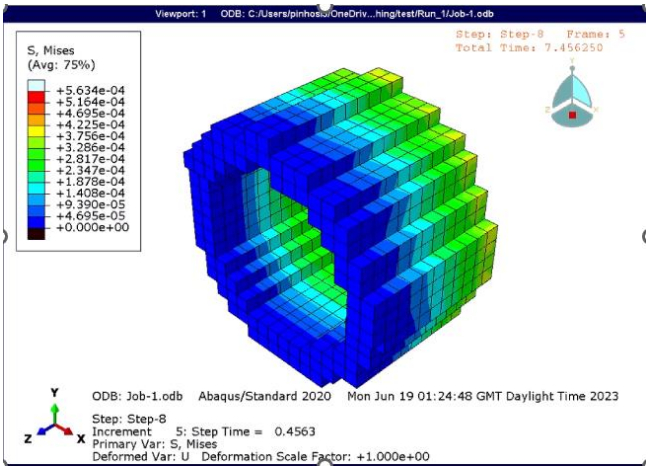


***Frame 3***

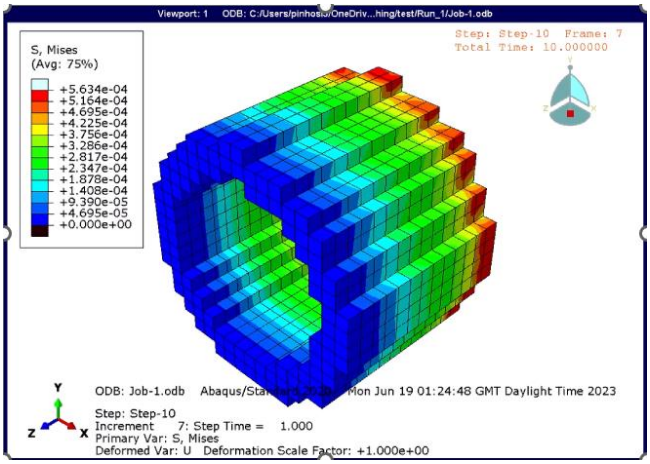


***Frame 4***

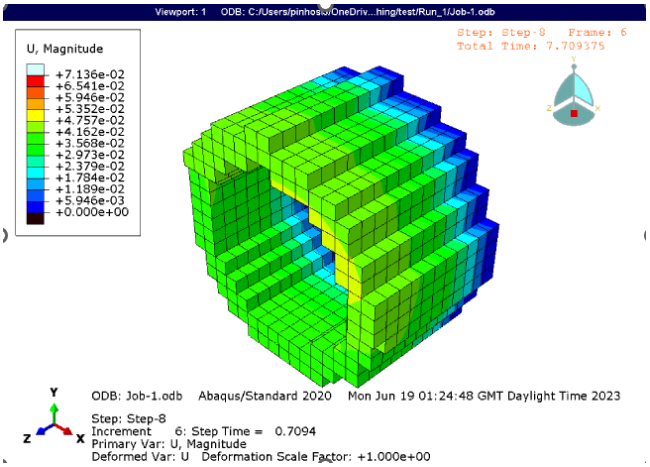


***Frame 3***

The same part is subjected to applied loads showing its magnitude on each layer.

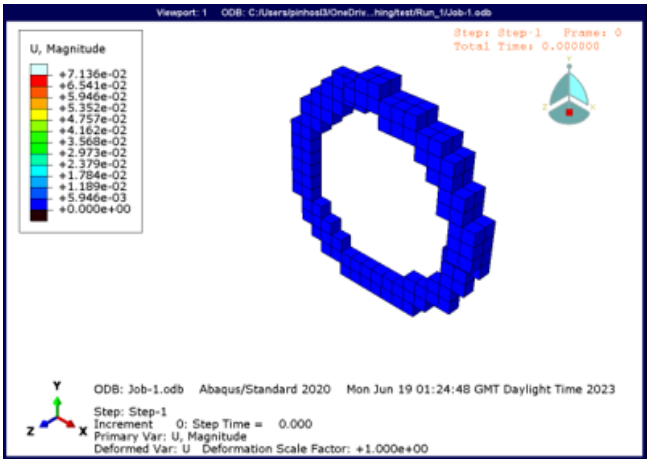


***Frame 1***

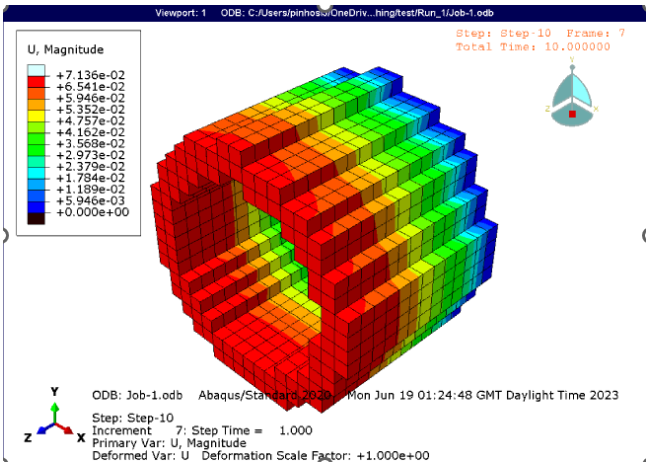


***Frame 4***

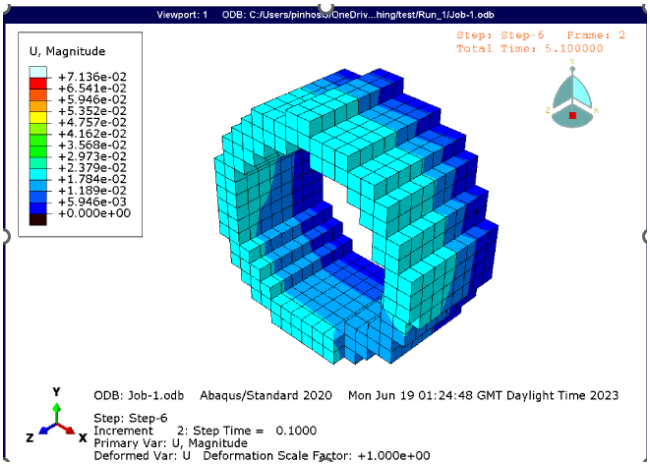


***Frame 2***

Printing speed is also simulated in Abaqus, two different scenario can be visualized in the following images:

**Scenario 1**: too fast printing speed.

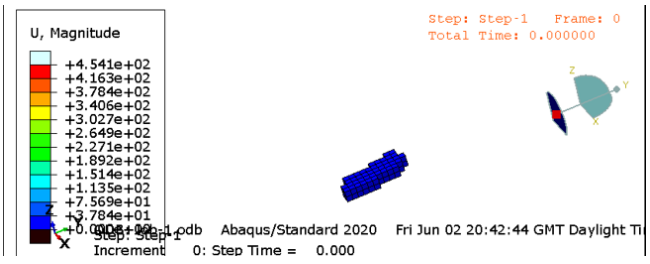


***Frame 1***

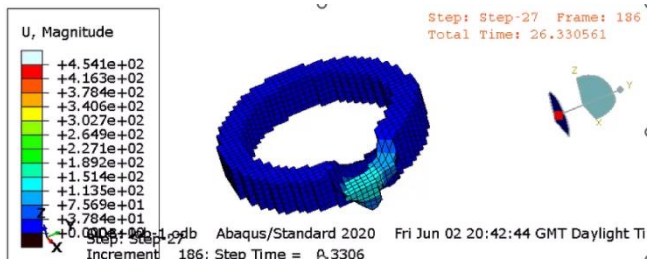


***Frame 2***

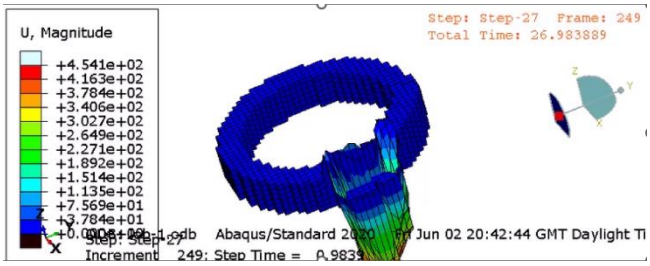


***Frame 3***

**Scenario 2**: adequate printing speed.

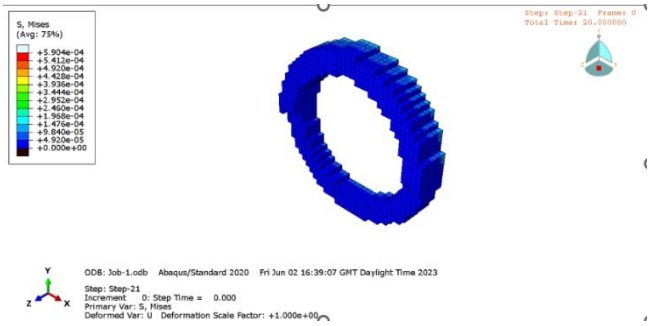


***Frame 1***

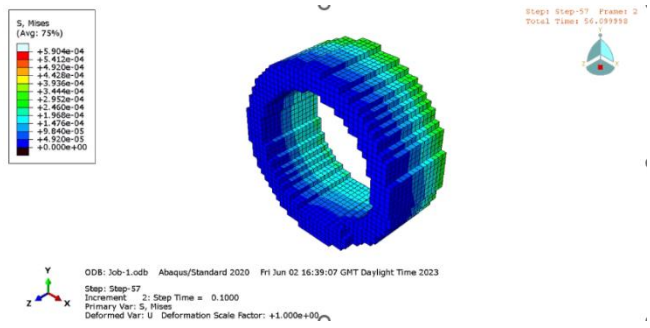


***Frame 2***

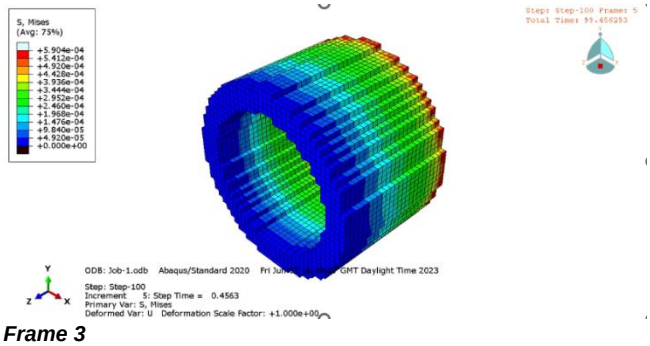


***Frame 3***

Once the simulations on a generic holed cylinder are verified, the topological optimisation is applied to geometry of the specimens.

Following the related diagrams:

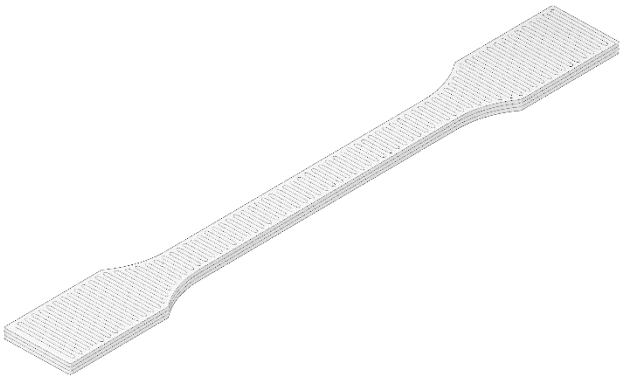

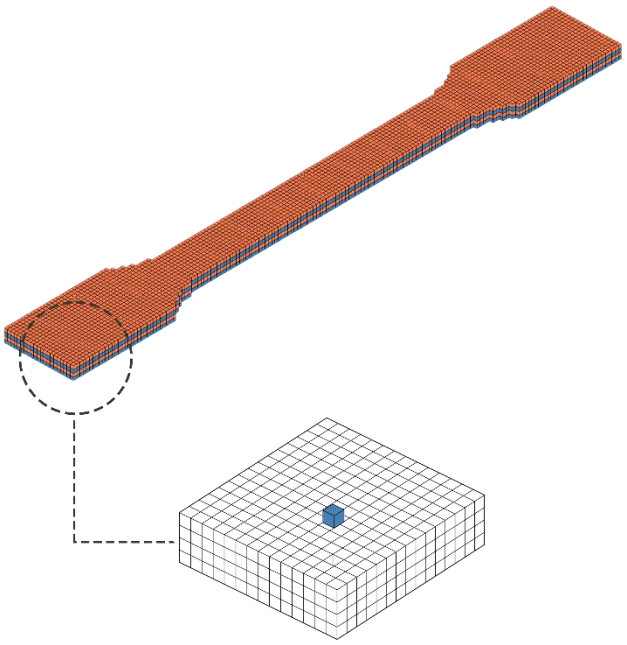


**Fig. 3.** *GH to Abaqus process. From top to bottom:*

- Computer-Aided Design *(create geometry and printing path).*
- Numeric Modelling *(Layer wise, mesh generation, contact-base interactions, defining time-dependent material properties, iterations, solver settings, generate input files).*

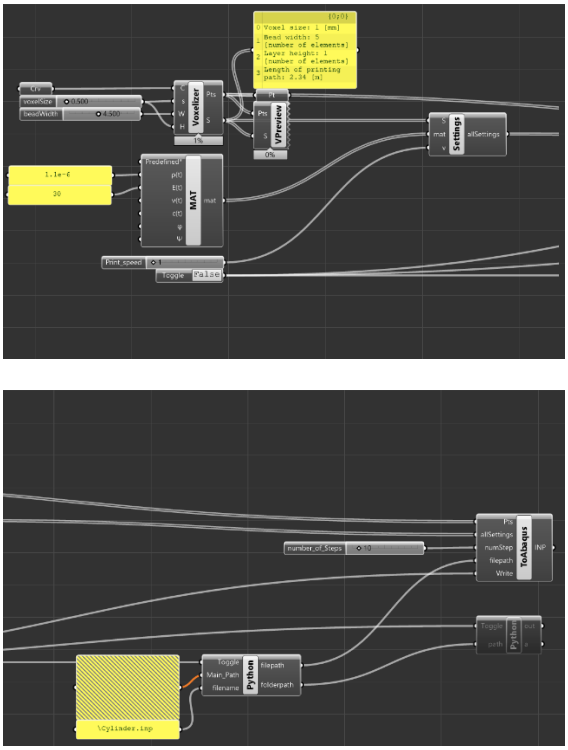


**Fig. 4.** *Grasshopper script, Concrete 3D Lab and Customed Python Component.*

This phase involves an interoperability between Concrete 3D Lab GH plugin to achieve a voxelization of the specimen which is consequently optimized in Abaqus.

The same process is applied to the structural column which is topological optimized by FEA in Abaqus after that Computer-Aided Design and Numeric Modelling methodology had been developed in Rhinoceros and Grasshopper 3D.

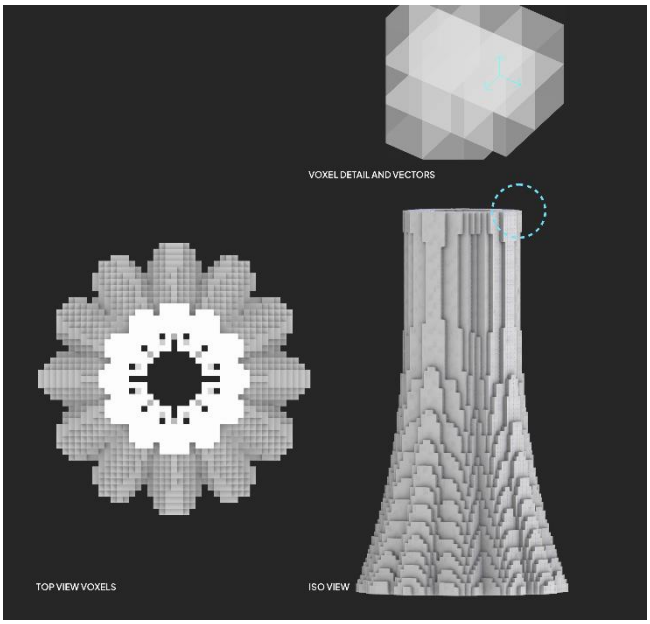


**Fig. 5.** *Numerical Modelling*.

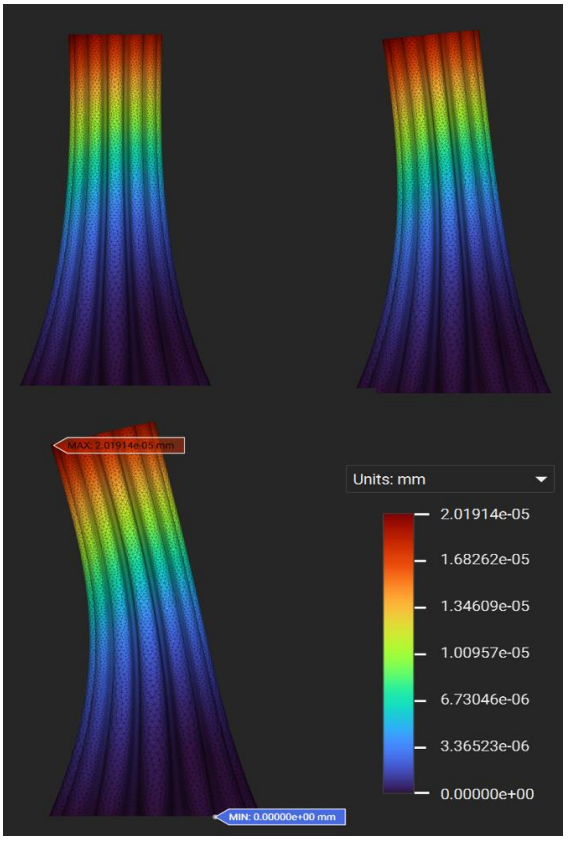


**Fig. 6.** *3D Part, FEA simulation, Columns.*

## Tensile test results

7 printing patterns were studied under tensile loading, namely, A-B-C-D-E-F and CS. The first 5 patterns were studied with 4, 6 and 12 layers while pattern F was done with 4, 8 and 12 layers and pattern CS had only 1 configuration. Each printing pattern was used to develop 3 specimens that were tested.

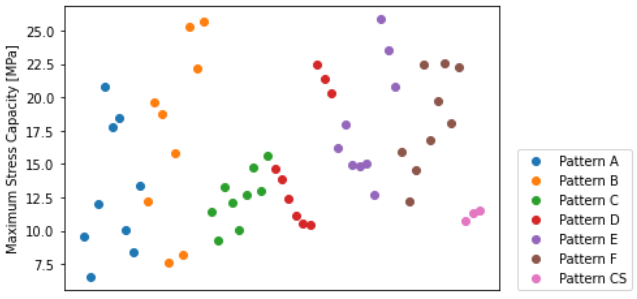


**Fig. 7:** Maximum stress capacity of coupon tests

It can be concluded that patterns E and F provide the most consistently high result. The next figures compare the average response of the 3 specimens for the same pattern varying the number of layers. Since this is an average plot, a sudden drop in the stress corresponds to one of the specimens failing.

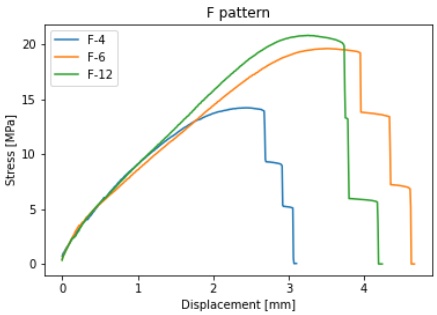


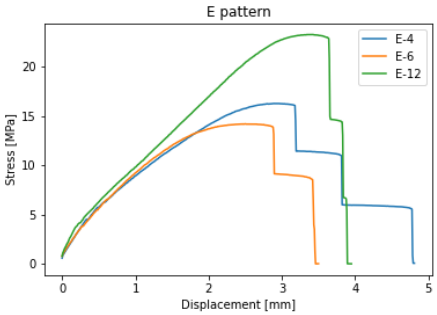


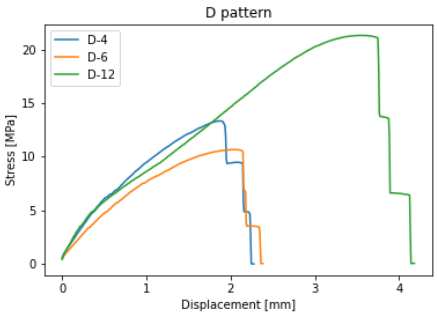


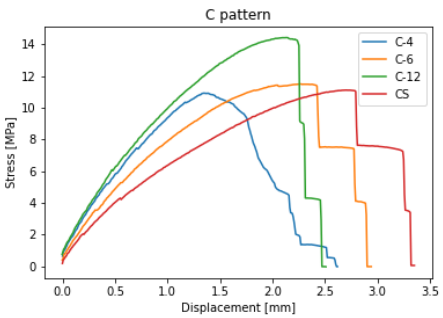


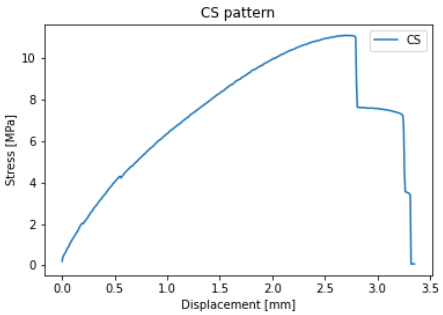


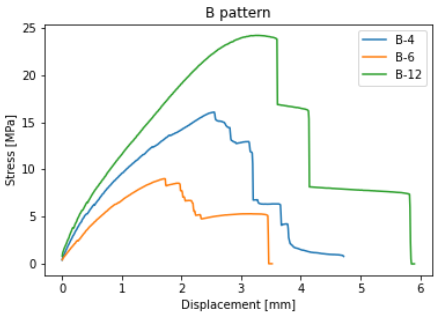


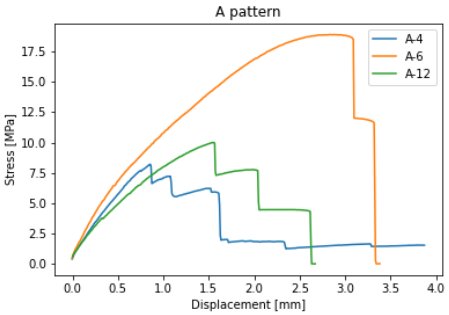


**Fig. 8.** *Average stress-displacement curve – Different patterns*

The next set of graphs compares different patterns for the same amount of layers. It can be concluded that 12 layers provides superior results than 4 layers and 6 layers. This could occur because, for the same cross-sectional dimensions of the coupons, more layers were obtained with smaller filament diameters:

- 0.95 mm *(4 layers height)*
- 0.58 mm *(6 layers height)*
- 0.41 mm (8 layers height)
- 0.26 mm *(12 layers height)*

Smaller filaments encourage greater bonding and smaller internal voids within the print, so commensurately better mechanical performance.

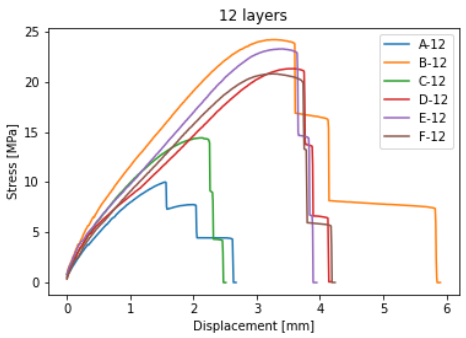


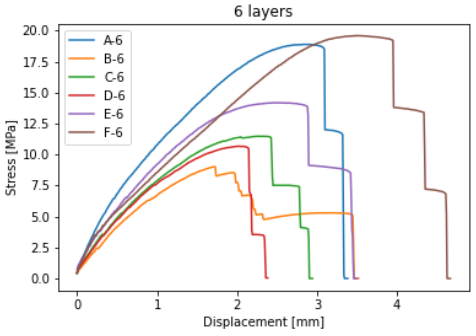

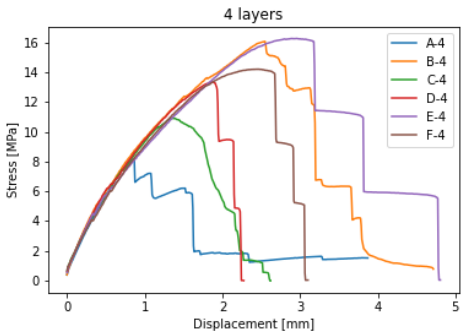


**Fig. 9.** *Average stress-displacement curve – Different layers*

The next graph shows if the difference in maximum stress capacity could be justified by a difference in mass. There is no correlation between the increase in mass (and therefore density) of the specimen and the increase of maximum stress capacity. Even by comparing the same patterns or the same number of layers, no correlation can be ascertained.

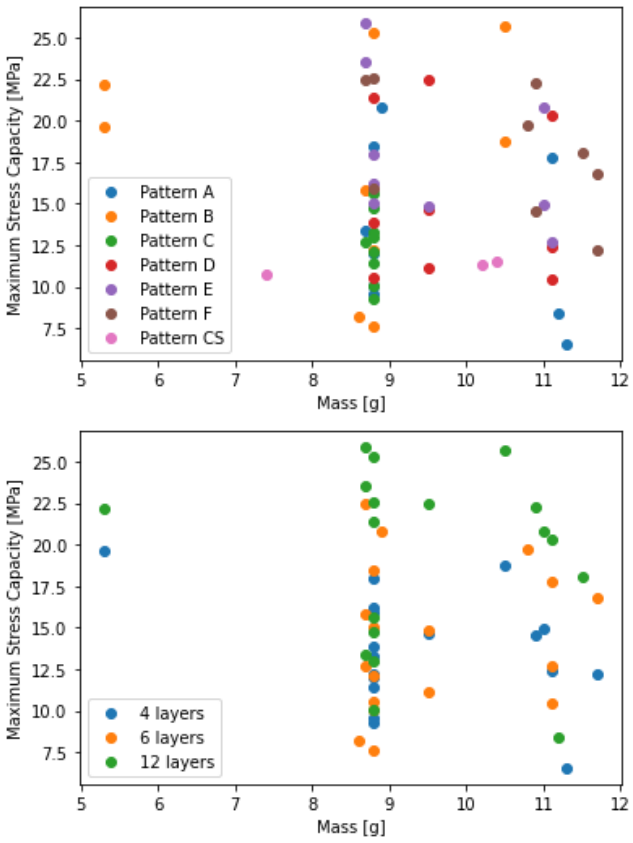


**Fig. 10.** *Impact of mass in the maximum stress capacity*

The next graph shows the correlation between maximum stress capacity and the average maximum height differences obtained from the microscope images. There is an acceptable correlation between the decrease in average maximum height differences of the specimen and the increase of maximum stress capacity. This demonstrates that further analysing the surface can lead to a better understanding of the ultimate capacity of 3D printed specimens.

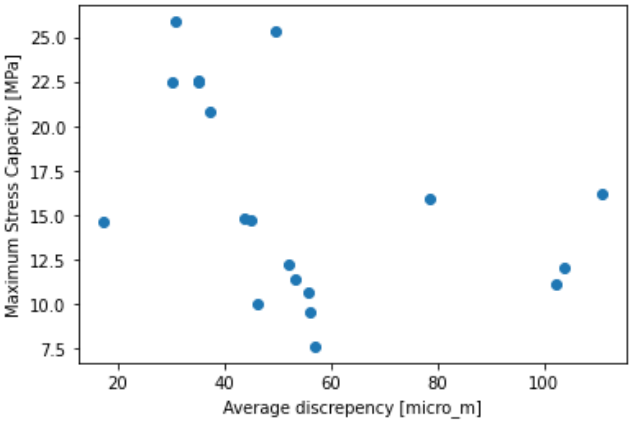


**Fig. 11.** *Impact of maximum height differences in the maximum stress capacity of the specimens*

## Neural Networks for Microscopic Surface Imaging

**A neural network architecture was developed in TensorFlow *(Python)* to predict the maximum stress capacity of the specimens from the images obtained from the microscope. The first step is to read the images, as shown in**

Fig. 2. 1 channel was used to read the images, considering only the data of surface height is registered.

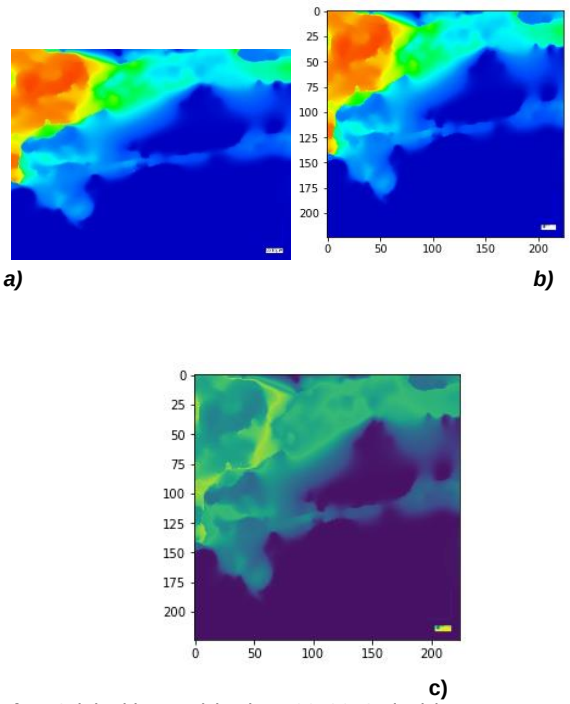

***a)*** ***b)*** **c)**

**a)** *Original image (size is 1536x2048 pixels).*
**b)** *Resized image (224x224 pixels) with 3 channels (Red, Green and Blue).*
**c)** *Image for the neural network. Size is 224x224 pixels and contains only 1 channel (in this case, colored as green). The scale at this stage is between 0 and 1.*

**Fig. 12.** Pre-processing of images from the microscope

After the images were scaled between 0 and 1, the data is rescale according to the values of the scale obtained from the microscope. In this way, the images are inputted to the Neural Network as matrices with the relative surface height at each point.

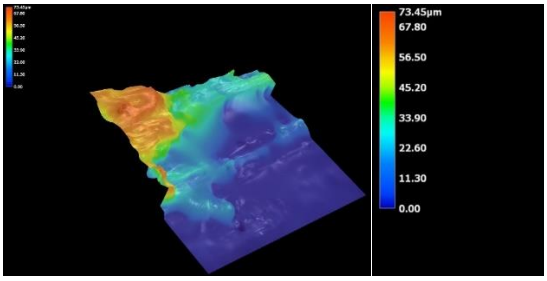


**Fig. 13.** Image from the microscope displaying its scale

Now that the images are ready to be inserted in a Neural Network, the next step is to associate the results from the tests (maximum stress capacity) with the images. Only 1 out of the 3 specimens was taken to the microscope, and 10 images were obtained for each of the 19 specimens, which gives 190 images to be analysed.

The architecture of the neural network was selected considering the trade-off between computational time and accuracy.

```
model = tf.keras.Sequential([
    tf.keras.layers.Conv2D(32, (3,3), activation='relu',  input_shape = (224,224,1)),
    tf.keras.layers.MaxPooling2D(2,2),
    tf.keras.layers.Conv2D(32, (3,3), activation='relu'),
    tf.keras.layers.MaxPooling2D(2,2),
    tf.keras.layers.Conv2D(32, (3,3), activation='relu'),
    tf.keras.layers.MaxPooling2D(2,2),
    tf.keras.layers.Flatten(),
    tf.keras.layers.Dense(128, activation='relu'),
    tf.keras.layers.Dense(1, activation='relu')])
```

**Fig. 14.** *Neural network architecture*

It should be noted that the input data is a 224x224 vector representing the relative height while the output is a scalar representing the tensile maximum capacity of those specimens. The dataset was separated between training, validation and testing data. In this case, 80% was used for training and 10% was used for validation and 10% for testing.

The neural network was trained for 50 epochs. Considering the results, the following graph shows the loss of the prediction function for each epoch.

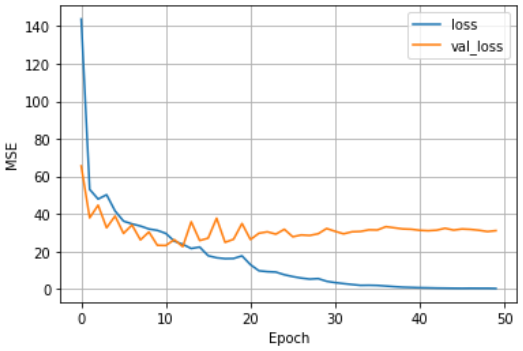


**Fig. 15.** *Evolution of training and validation loss during training*

It can be seen that, after epoch number 10, the model is experiencing overfitting. Even though the loss of the training data is decreasing (blue curve) the loss of the validation dataset is flat, which means the model is not generalizing outside the training dataset.

The following graphs prove this fact, where the training predictions *(fig. a)* and testing predictions *(fig. b)* are plotted. For a perfect prediction model, all the points should be over the *45* degree line.

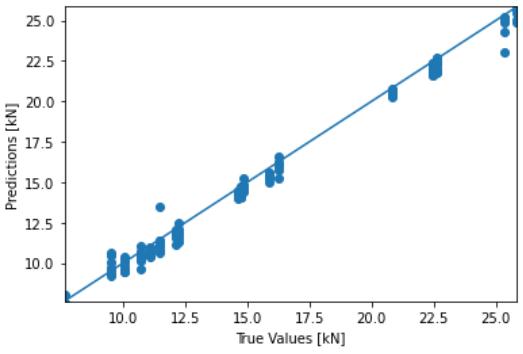


**a)**

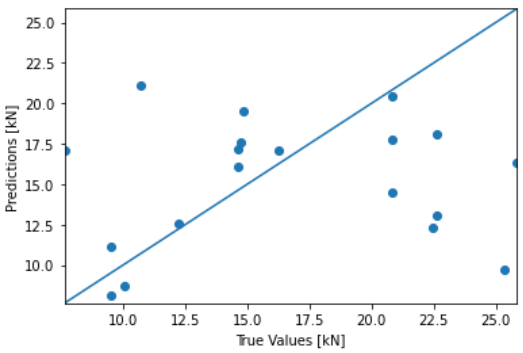


**b)**

**Fig. 16.** *Model capacity for predicting a) training data and b) test data*

The model is incapable of generalizing the predictions of maximum tensile strength from the images of the microscope. To improve this prediction, more data needs to be generated.

# 4 Robotic Manufacturing

## Geometry Definition and Data Generation for Robotic 3D Printing

Data-driven slicing and variable infills algorithms is used to define the tool pathing trajectory for the robotic arm with well-defined operational parameters acquired from digital microscope database.
From Kuka PRC (procedural robot control) in Grasshopper, the SRC and DAT files are exported and compiled for the robot.

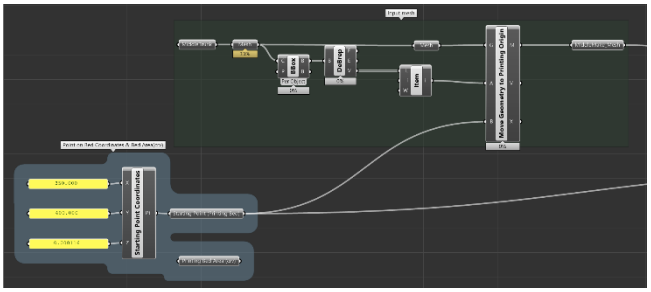

*Grasshopper script: importing the pathing trajectory and establishing the center of the printing bed.*

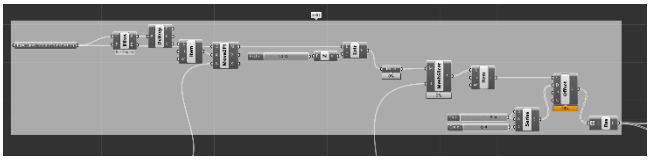

*Defining the skirt on the first layer.*

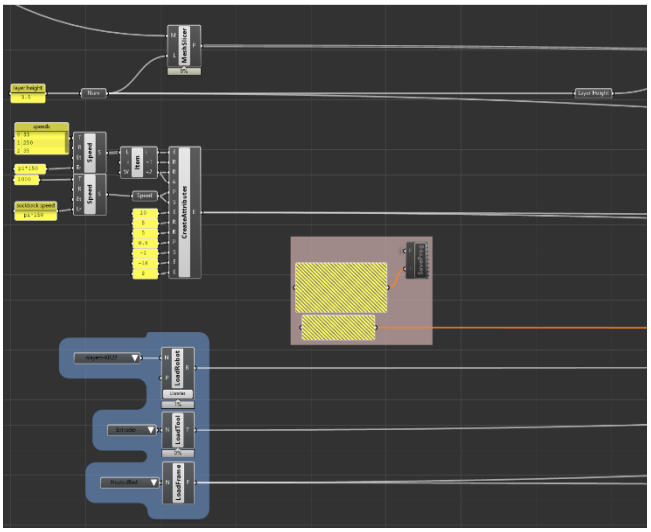

*Setting up the operation parameters for the robot.*

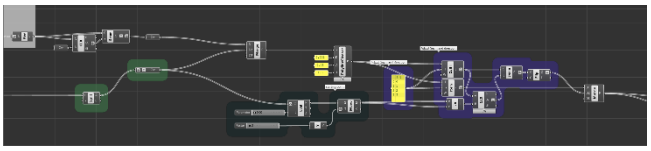

*Checking the starting printing point and path direction.*

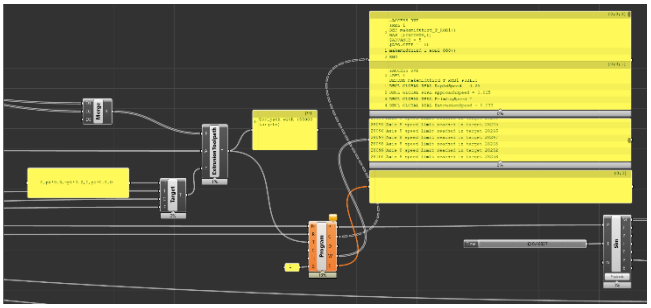

*Target initial position and pathing printing trajectory are input to the main program component.*

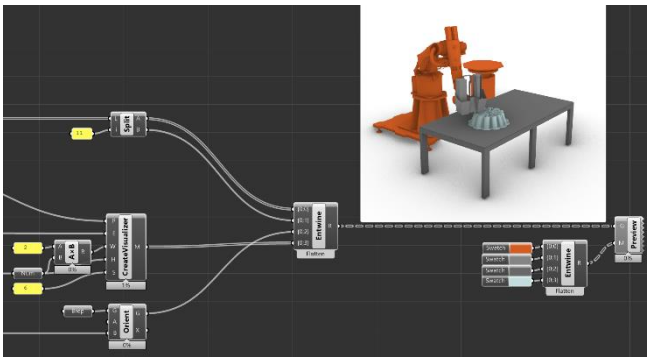

*Printing visualization.*

```
&ACCESS RVP
&REL 1
DEF makemidthird_T_ROB1_000()
$TOOL = TOOL_DATA[1]
$LOAD = LOAD_DATA[1]
$BASE = BASE_DATA[3]
ExtruderPos = $AXIS_ACT.E2
A = {A1 0,A2 -54,A3 126,A4 0,A5 -72,A6 0}
A.E1 = 0
A.E2 = ExtruderPos
PTP A
$OUT[1]=TRUE       ; Turn the extruder unit ON
WAIT FOR $IN[1]    ; Wait for extruder unit to reach the right
pressure
$ANOUT[1]= 0   ; Set airflow on festo valve default=0.08
$ANOUT[2]= 0    ; Set temperature on heat gun default=0.1
$VEL_EXTAX[2] = 100
$APO.CDIS = RapidZone
$VEL.CP = RapidSpeed
$VEL.ORI1 = 180
$VEL.ORI2 = 180
P = {X 816.654,Y 626.894,Z 8,A -14.1831,B 0,C 180}
P.E1 = 0
P.E2 = ExtruderPos
LIN P C_DIS
$VEL.CP = ApproachSpeed
P = {X 816.654,Y 626.894,Z 3,A -14.1831,B 0,C 180}
P.E1 = 0
P.E2 = ExtruderPos
LIN P
...
```

*SRC file of the 3D printed element.*

```
&ACCESS RVP
&REL 1
DEFDAT makemidthird_T_ROB1 PUBLIC
DECL GLOBAL REAL RapidSpeed = 0.25
DECL GLOBAL REAL ApproachSpeed = 0.035
DECL GLOBAL REAL PrimingSpeed = 1
DECL GLOBAL REAL ExtrusionSpeed = 0.033
DECL GLOBAL REAL SuckbackSpeed = 1
DECL GLOBAL REAL RetractionSpeed = 0.035
DECL GLOBAL REAL RapidZone = 5
DECL GLOBAL REAL ExtrusionZone = 10
DECL GLOBAL REAL ExtruderRate = -13.5
DECL GLOBAL REAL ExtruderPos = 0
DECL GLOBAL E6AXIS A
DECL GLOBAL E6POS P
ENDDAT
```

*DAT file of the 3D printed element.*

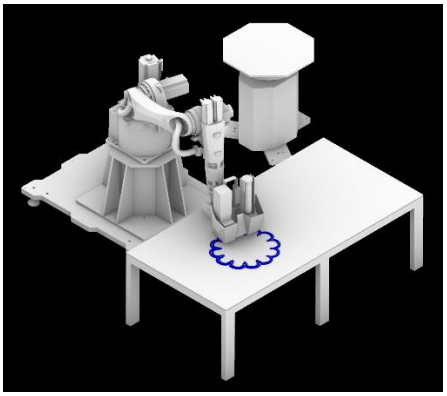

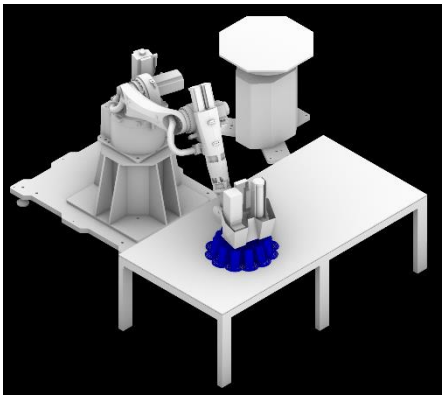

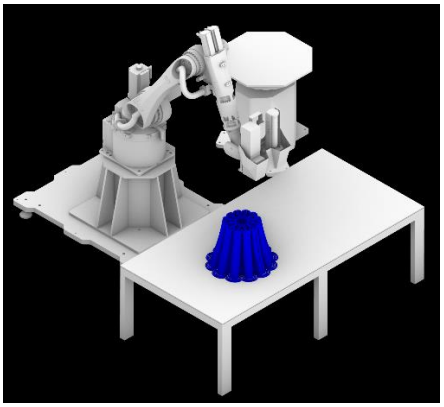

*Rhinoceros viewports, printing simulation*

# 5 Structural Testing

## 3D Part Testing at the Material Strength Lab

After a reliable printing process for the wood-base biopolymer has been delivered by material characterization and machine learning, samples topologically optimised in response to various loading and boundary conditions are printed and subjected to structural testing. Variances in material properties and microstructure will inform reliability analyses conducted in accordance with Eurocode EN 1990.

# 6 Conclusions

Investigating the of creation building structural parts using robotic 3D printing with wood-based biopolymers, the feasibility study identified that i) 3D printing processes for construction components in UK is at the early stages and it will require further investigation to explore which materials are suitable for AM processes and to comply with construction regulations, ii) there is a need for fundamental research to identify how the digital designed parts can be used for AM purposes, iii) to enable a transformational change and many variable part of AM processes and variety of construction business with the use of ML/AI there is the possibility to achieve good results, iv) establish a digital workflow and a database of material sample information is required for manufacturing sector and to develop Circular Economy strategies that can span across multiple industrial sectors.

The aim of the project is to create building structural parts using robotic 3D printing with wood-based biopolymers with high percentage of cellulose and fibres. The project looking contribute to familiarise architects and structural engineers with parametric design, coding and design for manufacturing using agile method of production such as robotic 3D printing. The project managed to determine a digital model for the mechanical properties of the cellulose polymer material through testing of 3D-printed coupons. Developed a machine learning algorithm for defect detection and material properties prediction based on microscopic pattern data although the amount a data sample data should be much more to achieve sustainable results.
We successfully establish a digital workflow in order to simulate offline the 3D printing and deposition process and to enable digital twin environment and digital demonstrated the structural performance of prototype 3D-printed part. The digital twin model was develop with a material deposition simulation, calculation the inverse kinematic of the robot arm and definition of 3D printing parameters with ML algorithm through material sample.

The project will certainly showed the potential of 3D printing in the construction process, the definition of digital twin model to reduce cycle times and the potential of ML for digital manufacturing processes.

# 7 References


[1] Smith, L. (2021). Plastic waste – Briefing Paper 08515, 13/04/2021, HoC Library.
[2] Wu, Z., Wang, X., Zhao, X., Noori, M. (2014). State-of-the-art review of FRP composites for major construction with high performance and longevity. *Intern. J. Sust. Mat. & Struct. Sys.*, 1(3):201-231.
[3] Paolini, A., Kollmannsberger, S., Rank, E. (2019). Additive manufacturing in construction: A review on processes, applications, and digital planning methods. *Additive Manufacturing*, 30:100894.
[4] McCann, F., Rossi, F. (2021). Investigating local buckling in highly slender elliptical hollow sections using 3D-printed analogues. CIMS2020, 11/07/21, Poland.
[5] Rossi, F. (2018). Fibre Wonder (DARLAB research monograph), London.
[6] Gieljan Vantyghem, Ticho Ooms, Wouter De Corte, VoxelPrint: A Grasshopper plug-in for voxel-based numerical simulation of concrete printing, Automation in Construction, Volume 122, 2021, 103469, ISSN 0926-5805,


# 8 Feasibility Study Team Members

The study was conducted by a team of researchers from **London South Bank University.**


**Federico Rossi**, Associate Professor (PI)
**Finian McCann**, Associate Professor (Co-PI)
**Luis Santos**, Senior Lecturer (ECR)
**Daniele Ferrentino**, Research Associate (ECR)

# connected everything.

industrial systems in the digital age

Connected Everything
Faculty of Engineering University of Nottingham
University Park Nottingham NG7 7RD UK
www.connectedeverything.ac.uk